Nonlinear Electron Paramagnetic Resonance Studies of the Interaction of Cytochrome *c* Oxidase with Spin-Labeled Lipids in Gel-Phase Membranes[†]

Tibor Páli,[‡,§] Jörg H. Kleinschmidt,[‡,||] Gary L. Powell,[⊥] and Derek Marsh*,[‡]

Max-Planck-Institut für biophysikalische Chemie, Abteilung Spektroskopie, D-37070 Göttingen, Germany, and Department of Biological Sciences, Clemson University, Clemson, South Carolina 29634-1903.

ABSTRACT: The interaction of lipids, spin-labeled at different positions in the *sn*-2 chain, with cytochrome *c* oxidase reconstituted in gel-phase membranes of dimyristoylphosphatidylglycerol has been studied by electron paramagnetic resonance (EPR) spectroscopy. Nonlinear EPR methods, both saturation transfer EPR and progressive saturation EPR, were used. Interaction with the protein largely removes the flexibility gradient of the lipid chains in gel-phase membranes. The rotational mobility of the chain segments is reduced, relative to that for gel-phase lipids, by the intramembranous interaction with cytochrome *c* oxidase. This holds for all positions of chain labeling, but the relative effect is greater for chain segments closer to the terminal methyl ends. Modification of the paramagnetic metal-ion centers in the protein by binding azide has a pronounced effect on the spin−lattice relaxation of the lipid spin labels. This demonstrates that the centers modified are sufficiently close to the first-shell lipids to give appreciable dipolar interactions and that their vertical location in the membrane is closer to the 5-position than to the 14-position of the lipid chains.

Cytochrome *c* oxidase is the terminal member of the mitochondrial respiratory chain that effects the reduction of molecular oxygen to water by means of electrons donated from reduced cytochrome *c*. The reaction involves pumping protons toward the cytosol to provide the chemiosmotic driving force for ATP synthesis. The cytochrome *c* oxidase enzyme from beef heart is a multisubunit polytopic transmembrane protein, which contains several metal-ion centers that are designated heme *a*, heme a_3, Cu_A, and Cu_B. The crystal structure of the whole 13-subunit assembly of the bovine enzyme has been determined (*1*) and further refined recently for different redox forms (*2*).

As a representative large integral membrane protein, cytochrome *c* oxidase has been the subject of several studies of lipid−protein interactions (*3−6*) by spin-label EPR[1] methods. The latter has proved to be particularly useful for quantitating the lipid−protein interactions with a wide variety of intrinsic proteins in fluid-phase membranes (for a recent review see ref *7*). Far less information is available on lipid−protein interactions in gel-phase lipid membranes. These not only are found in reconstituted systems but also may be

considered as generally representative of membrane regions with high lipid packing densities, e.g., in spatially segregated membrane domains (*8*). The few magnetic resonance studies that concentrate on lipid−protein interactions in gel-phase membranes include ^{2}H NMR studies of rhodopsin (*9*) and saturation-transfer electron paramagnetic resonance (ST-EPR) of the myelin proteolipid protein (*10*) in reconstituted membrane systems. Nonlinear EPR methods (ST-EPR and also progressive saturation EPR) are well suited to such investigations with spin-labeled lipids. This is because both the gel-phase bilayer membrane lipids and the lipids interacting directly with the intramembrane surface of the integral protein have rotational motions on a time scale to which these T_1-dependent methods are optimally sensitive (*11*).

In the present work, we have studied lipid−protein interactions with bovine cytochrome *c* oxidase that is reconstituted in gel-phase dimyristoylphosphatidylglycerol (DMPG) as the host membrane lipid. Phosphatidylglycerol is taken as representative electrostatically of the negatively charged lipid component of the inner mitochondrial membrane (predominantly diphosphatidylglycerol). Lipid−protein interactions between cytochrome *c* oxidase and DMPG were characterized recently in fluid-phase membranes (*12*). Here,

* Corresponding author: Tel +49-551-201 1285; FAX +49-551-201 1501; E-mail dmarsh@gwdg.de.

[‡] Max-Planck-Institut für biophysikalische Chemie.

[§] Permanent address: Institute of Biophysics, Biological Research Centre, H-6701 Szeged, Hungary.

[||] Present address: Department of Molecular Physiology & Biological Physics, Health Sciences Center, University of Virginia, Charlottesville, VA 22906-0111

[⊥] Clemson University.

[1] Abbreviations: DMPG, 1,2-dimyristoyl-*sn*-glycero-3-phosphoglycerol; *n*-PGSL, 1-acyl-2-[*n*-(4,4-dimethyl-*N*-oxy-2-oxazolidinyl)stearoyl]-*sn*-glycero-3-phosphoglycerol; *n*-SASL, *n*-(4,4-dimethyl-*N*-oxy-2-oxazolidinyl)stearic acid; cyt ox, cytochrome *c* oxidase; HEPES, 4-(2-hydroxyethyl)-1-piperazineethanesulfonic acid; EDTA ethylenediaminetetraacetic acid; EPR, electron paramagnetic resonance; ST-EPR, saturation transfer electron paramagnetic resonance; V_1, first-harmonic absorption electron paramagnetic resonance spectrum detected in phase with respect to the static magnetic field modulation; V_2', second-harmonic absorption electron paramagnetic resonance spectrum detected 90°-out-of-phase with respect to the static magnetic field modulation.

we have used both ST-EPR and progressive saturation EPR, together with phosphatidylglycerol probes (*n*-PGSL) that are spin-labeled at different positions in the *sn*-2 chain, for studies in gel-phase membranes. Because cytochrome *c* oxidase contains endogeneous paramagnetic metal centers, the nonlinear spin-label EPR spectra are sensitive not only to the rotational dynamics of the lipid chains but also to spin–spin interactions with these metal-ion centers. Significant and consistent effects are obtained on modifying the metal centers by binding azide. These latter results demonstrate a direct interaction with the spin-labeled lipid chains at the intramembrane perimeter of the protein.

MATERIALS AND METHODS

Materials. DMPG was obtained from Avanti Polar Lipids (Alabaster, AL), and was found to be pure on thin-layer chromatography with the solvent system $CHCl_3/CH_3OH/$ ammonia (65/30/3 v/v/v). Phosphatidylglycerol spin labels with the nitroxyl group on the *n*th carbon atom of the *sn*-2 acyl chain (*n*-PGSL, *n* = 4, 5, 7, 12, or 14) were synthesized from the corresponding spin-labeled stearic acids (*n*-SASL), as described in ref *13*. Cytochrome *c* oxidase (cyt ox) was prepared from beef heart by the method of Yu et al. (*14*), with the modifications given in ref *15*. Lipid substitution by DMPG was carried out in a manner similar to that described in ref *16* for the substitution by dimyristoylphosphatidylcholine. Cytochrome *c* oxidase was treated with a 500-fold molar excess of DMPG in 10 mM HEPES buffer, pH 7.4, containing 1 mM EDTA, for 1 h at room temperature. The buffer contained 0.2% sodium cholate to facilitate the lipid exchange. After the solution was cooled on ice, the enzyme was precipitated by adding cold concentrated ammonium sulfate solution to a final concentration of 35%. The supernatant was removed after centrifugation at 4 °C; then the lipid incubation and ammonium sulfate precipitation steps were performed a second time. Subsequently, the cyt ox was taken up in buffer containing 1% sodium cholate, and centrifuged at 66000*g* (4 °C). The supernatant was assayed for protein and lipid content by Lowry (*17*) and phosphate (*18*) assays, respectively.

Reconstitution and ESR Sample Preparation. The final cyt ox-containing solution in cholate was divided into several aliquots, and appropriate amounts of DMPG were added to each aliquot to give the desired molar ratios of DMPG to cyt ox. For cholate removal, samples were dialyzed at 4 °C against 10 mM HEPES buffer, pH 7.4, containing 1 mM EDTA, and 1 M KCl. The dialysis buffer was changed after 8–12 h, for a total of 3 times. Reconstituted membrane samples were found to be homogeneous on continuous sucrose-density gradients. Cytochrome oxidase activity after reconstitution was measured according to Yonetani (*19*). An activity of $A = 5107$ min^{-1} was found, i.e., approximately half of that before the reconstitution ($A = 11\,000$ min^{-1}). Activity after reconstitution in DMPG was therefore roughly comparable to the activity after reconstitution with other phospholipids (cf. ref *14*). After dialysis, each sample was spin-labeled from a concentrated solution of *n*-PGSL in ethanol, which was such that the total amount of ethanol did not exceed 1% of the total sample volume and the final spin-label concentration was 1 mol % of the total lipid. After washing to remove unincorporated spin label, membranes were recentrifuged, taken up in a small volume of buffer,

and transferred into EPR capillaries. The samples were then packed as pellets in the capillaries by using a benchtop centrifuge. EPR spectra were recorded after removal of the excess supernatant from the sample capillaries. All EPR samples were analyzed for their lipid and protein content after the spectra had been recorded. Lipid/protein ratios were determined by Lowry protein assays (with bovine serum albumin as standard) and Rouser phosphate assays (*17, 18*). Except for the period of measurement, samples were always kept on ice (or at 4 °C during centrifugation).

EPR Spectroscopy. EPR spectra were recorded at 10 °C on a Varian 9-GHz spectrometer (model E-12 Century Line; Varian, Sunnyvale, CA) equipped with a TE102 rectangular cavity (Varian). Temperature was controlled to within ±0.1 °C by using nitrogen gas-flow temperature regulation and was measured with a fine-wire thermocouple positioned at the top of the sample within the EPR capillary. EPR sample capillaries (1 mm i.d.) were accommodated in a 4-mm quartz EPR tube that contained light silicone oil for thermal stability. A custom-built sample holder allowed positioning of the sample in the cavity with an accuracy of 0.1 mm. The spectrometer was interfaced to an IBM personal computer with a Tecmar Labmaster A/D converter for digitizing and storing the measured EPR data. For improved sensitivity, spectra were accumulated 8–16 times, depending on the signal-to-noise ratio. For conventional EPR spectra, the field modulation frequency was 100 kHz with a modulation amplitude of 1.25 G. A filter time constant of 0.25 s was used. Saturation transfer and progressive saturation experiments were performed with samples trimmed to 5 mm length that were centered in the microwave cavity. Calibration and measurement of H_1 field intensity and determination of cavity Q were performed as described in ref *20*. All saturation measurements were performed under critical coupling conditions. ST-EPR spectra were recorded in the second-harmonic, absorption mode (V_2' display), with the lock-in detector set at 90°-out-of-phase by the self-null method. The modulation frequency was 50 kHz (detection at 100 kHz), modulation amplitude was 5.0 G, and rms H_1 field at the sample was 0.25 G (*21*). Progressive saturation EPR spectra were analyzed in terms of the double integral (*22*), and ST-EPR spectra were analyzed by both the line height ratio (*23*) and first integral (*24*) methods. Calibrations of rotational correlation times for ST-EPR spectra were taken from ref *24*, as given in ref *25*.

RESULTS AND DISCUSSION

Chemical Lipid–Protein Reactions. Direct evidence for an interaction between the spin-labeled lipid and the cytochrome *c* oxidase protein comes from measurements of the rates of reduction of the spin-label nitroxyl free radical in reconstituted membranes in the fluid phase. The time-dependent decay of the EPR intensity obtained from 14-PGSL in DMPG/cyt ox membranes at 36 °C is shown in Figure 1. This time-dependent decrease in intensity arises from chemical reduction of the nitroxide by reducing centers localized on the protein. The reaction is to some extent diffusion-controlled because the EPR intensity is quite stable at lower temperatures in the gel phase, where lipid translational diffusion is very slow. The localized nature of the reaction is evident from the fact that the reaction rate is dependent on the position, *n*, of the spin label group in the
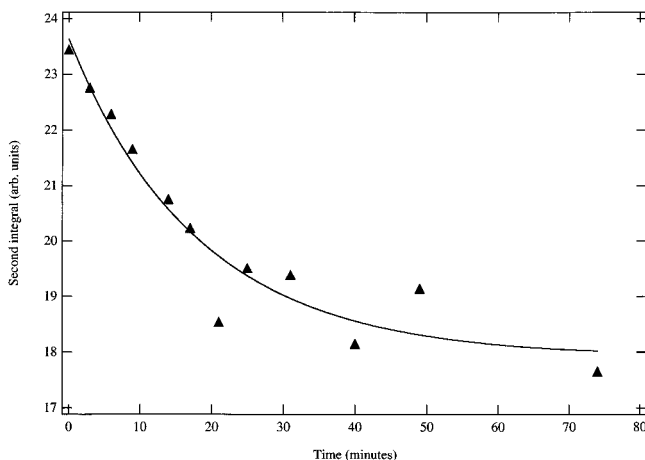
FIGURE 1: Decay of the double-integrated intensity of the conventional EPR spectrum of 14-PGSL spin label in cytochrome *c* oxidase/DMPG complexes (1:150 mol/mol), measured at pH = 7.4 and T = 36 °C. Solid line indicates a best-fitting single exponential with a rate constant of 0.054 min^{-1}.
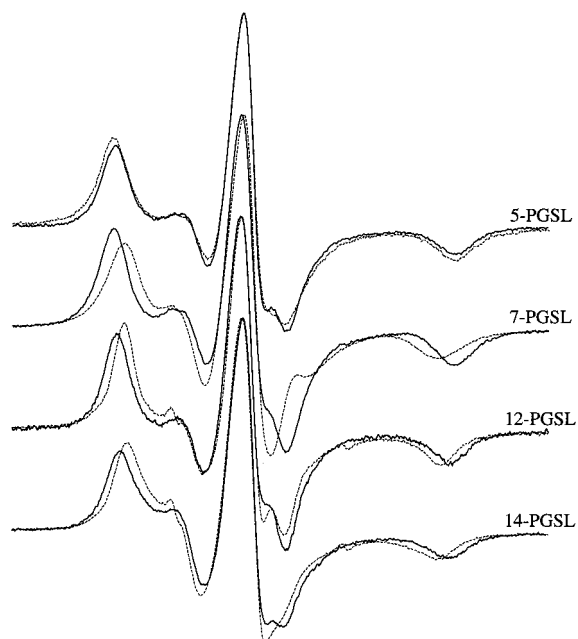

FIGURE 2: Conventional EPR spectra (V_1 display), measured at low microwave power (H_1 = 0.083 G), from *n*-PGSL spin labels in aqueous dispersions of DMPG alone (---) and in cytochrome *c* oxidase/DMPG complexes (—) at 10 °C. The position, *n*, of the spin label in the *sn*-2 chain of the different *n*-PGSL positional isomers is indicated on the figure. Lipid:protein ratio = 53 mol/mol. Total scan width = 100 G.

lipid chain. The rate is fastest for 14-PGSL and considerably slower for spin labels located further up the chain (data not shown). Fitting to a single exponential, as shown in Figure 1, results in a decay rate of 0.054 min^{-1} for 14-PGSL.

Conventional EPR Spectra in the Gel Phase. The V_1 EPR spectra of different *n*-PGSL spin label positional isomers at 10 °C, in the gel phase of DMPG, are given in Figure 2. Solid lines are the spectra from DMPG/cyt ox complexes with similar lipid/protein ratios of ca. 50:1 mol/mol. Dashed lines are the corresponding spectra from aqueous dispersions of DMPG alone. In all cases, the outer hyperfine splittings, $2A_{max}$, of the spectra are greater in the lipid/protein complexes than they are in membranes of the gel-phase lipid alone. This corresponds to a higher degree of immobilization of the lipid
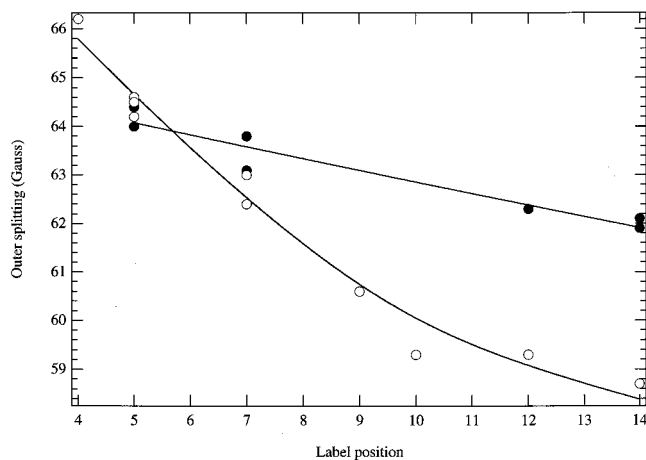

FIGURE 3: Positional dependence (*n*) of the outer hyperfine splitting, $2A_{max}$, in the low-power EPR spectra of *n*-PGSL spin labels in aqueous dispersions of DMPG (○) and in cytochrome *c* oxidase/DMPG complexes (●) at 10 °C.

chains in the lipid/protein complexes. The degree of immobilization of the lipid chain depends, however, on the segment, *n*, of the chain to which the spin label is attached.

The dependence of the outer hyperfine splitting on chain segment position is given in Figure 3 for DMPG membranes with and without incorporated cytochrome *c* oxidase protein. In normal gel-phase lipid bilayers, the chains exhibit a characteristic, although limited, gradient of increasing flexibility toward the terminal methyl ends (*26*). This is evident from the decreasing values of A_{max} in DMPG alone that are shown in Figure 3. The effect of the membrane-spanning protein is to reduce this flexibility gradient considerably. It is likely that the major restriction of the flexibility arises from lipid chains directly in contact with the intramembranous surface of the protein. This has been found previously to be the case for spin-labeled lipids interacting with rhodopsin in rod outer segment disk membranes (*27*). In the gel phase, the lipid chain environment immediately adjacent to the protein is not readily distinguished from that in the bilayer regions of the membrane remote from the protein (cf. ref *10*). This is unlike the situation in the fluid phase, but the possibility still exists that these environments are distinct, although unresolved, in gel-phase membranes.

Saturation Transfer EPR Spectra in the Gel Phase. Figure 4 gives the V_2' ST-EPR spectra that correspond to the conventional V_1 EPR spectra that were presented in Figure 2. Comparison with the latter shows a considerably greater effect of the protein on the microsecond motions of the lipid chains, to which ST-EPR is sensitive, than on the nanosecond motions to which conventional EPR is sensitive (see, e.g., ref *28*). Values for the effective rotational correlation times, τ_R^{eff}, of the *n*-PGSL spin labels were obtained from the diagnostic line height ratios (L''/L, C'/C, and H''/H) in the low-, central-, and high-field regions of the ST-EPR spectra (see ref *23* for a definition of ST-EPR line height ratios). For this purpose, calibrations obtained with spin-labeled hemoglobin in aqueous media of different viscosities were used (*25, 29*):

$$\tau_R^{eff}(P) = \frac{k}{P_0 - P} - b \qquad (1)$$

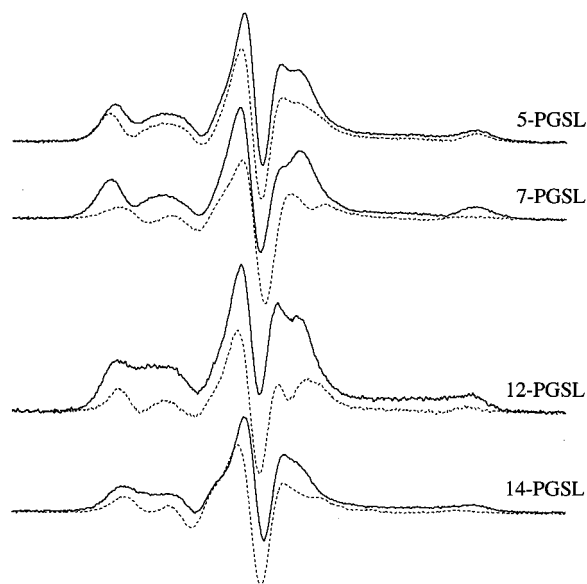where P_0 is the maximum, rigid-limit value of line height

FIGURE 4: Second harmonic, 90° out-of-phase ST-EPR spectra (V_2' display) from *n*-PGSL spin labels in aqueous dispersions of DMPG alone (---) and in cytochrome *c* oxidase/DMPG complexes (—) recorded at 10 °C. The position, *n*, of the spin label in the *sn*-2 chain of the different *n*-PGSL positional isomers is indicated on the figure. Lipid:protein ratio = 53 mol/mol. Total scan width = 100 G.

Table 1: Effective Rotational Correlation Times[a]

spin label	L''/L	$\tau_R^{eff}(L)$ (μs)	C'/C	$\tau_R^{eff}(C)$ (μs)	H''/H	$\tau_R^{eff}(H)$ (μs)
			DMPG Alone			
4-PGSL	0.681	28	0.017	5	0.519	36
5-PGSL	0.644	26	−0.611	<0.1	0.467	29
7-PGSL	0.230	2.4	−1.517	<0.1		
12-PGSL	0.478	15	−0.759	<0.1	0.438	25
14-PGSL	0.428	12	−1.099	<0.1	0.300	8
			DMPG/Cytochrome *c* Oxidase			
5-PGSL	0.725	32	−0.221	2	0.677	63
7-PGSL	0.626	24	−0.302	1	0.580	46
12-PGSL	0.814	41	0.044	5	0.663	60
14-PGSL	0.700	30	−0.309	1	0.619	52

[a] $\tau_R^{eff}(P)$ values were obtained from diagnostic ST-EPR line height ratios, P'/P, for *n*-PGSL spin labels in aqueous DMPG dispersions and in DMPG/cyt ox (50:1 mol/mol) complexes at 10 °C. Rotational correlation times were obtained by use of calibrations with spin-labeled hemoglobin (*25, 29*).

ratio *P* and *k* and *b* are calibration constants that are given in ref *25*. These derived values of effective correlation time are given in Table 1 for DMPG bilayers with and without cytochrome *c* oxidase.

In gel-phase bilayers alone, the rotational correlation times are evidently anisotropic, because the three diagnostic regions of the ST-EPR spectra produce different values, relative to isotropically rotating hemoglobin (see Table 1). Effective rates of rotation are considerably faster about the long axis of the lipid molecules to which only the C'/C ratio is sensitive (*30, 31*). The rates of off-axial chain rotation that are recorded by the line height ratios, L''/L and H''/H, in the outer diagnostic regions of the spectra are considerably slower. Comparable values are obtained from these two ratios, indicating relatively little anisotropy in the off-axial rotation (see also ref *32*). Somewhat atypical, i.e., nonsystematic, results are obtained for the 7-PGSL spin label that is situated

Table 2: Normalized Integrated ST-EPR Intensities[a]

spin label	$I_{ST,P}$ ($\times 10^2$)	$I_{ST,L}$ ($\times 10^2$)
5-PGSL	0.43	0.21
7-PGSL	0.28	0.02
12-PGSL	0.52	0.08
14-PGSL	0.37	0.07

[a] I_{ST} values (defined in ref *24*) of the ST-EPR spectra from *n*-PGSL spin labels in DMPG bilayers ($I_{ST,L}$) and in DMPG/cyt ox (50:1 mol/mol) complexes ($I_{ST,P}$) at 10 °C are given.

toward the center of the lipid chain. This anomaly almost certainly arises from the known tendency of lipids labeled in this region of the chain to segregate in gel-phase membranes (*33*). With this exception, the ST-EPR correlation times reflect the gradient of increasing flexibility toward the terminal methyl ends of the chains that was evident in the conventional EPR spectra. This is fully in agreement with previous ST-EPR studies on gel-phase phosphatidylcholine lipids (*26*).

Incorporation of cytochrome *c* oxidase in gel-phase DMPG membranes gives rise to a slowing in rate of both axial and off-axial chain rotational motion. An analogous effect has been found previously with the myelin proteolipid protein, for overall chain mobility in gel-phase lipid membranes (*10, 11*). The present results display a very pronounced effect on the chain flexibility profile for microsecond motions. Again with the exception of the anomalous 7-position label, the flexibility gradient is almost entirely removed by the presence of the transmembrane protein. The effective rotational correlation times for 14- and 12-PGSL are comparable to those for 5-PGSL. Compared with gel-phase lipids alone, the protein therefore restricts the chain flexibility to a much greater extent at the terminal methyl ends than it does for positions closer to the lipid headgroups. The effective rotational correlation times deduced from the L''/L and H''/H diagnostic ratios differ somewhat in the presence of cytochrome *c* oxidase. This is unlike the situation for DMPG membranes alone, which suggests that lipid−protein interaction induces some anisotropy in the off-axial chain motions.

Saturation Transfer EPR Intensities. Further information on the lipid−protein interaction is obtained from the integrated intensities of the ST-EPR spectra from the spin-labeled lipids. This spectral parameter is sensitive not only to rotational mobility but also to any interactions that affect the spin−lattice (i.e., T_1) relaxation of the spin label (see, e.g., ref *34*). The normalized integrated ST-EPR intensities, I_{ST}, of the different *n*-PGSL spin labels in gel-phase DMPG membranes and in DMPG/cyt ox complexes are given in Table 2. Progressive changes are seen in the values of I_{ST} with position, *n*, of the spin label in the lipid chain for the DMPG membranes. This yet again reflects the chain flexibility gradient in gel-phase bilayer membranes. The one exception is the 7-PGSL spin label, for which the integrated ST-EPR intensities are anomalously low, because they are reduced by spin−spin interactions between the partially segregated labels (see ref *35*) in both membrane systems.

For all positions of labeling, the integrated ST-EPR intensities are much higher in the presence of cytochrome *c* oxidase than they are in the absence of the protein (see Table 2). Because the lipid/protein ratio is close to the number of first-shell boundary lipids (cf. ref *12*), the values of $I_{ST,P}$ given in Table 2 directly reflect the properties of the lipid−protein
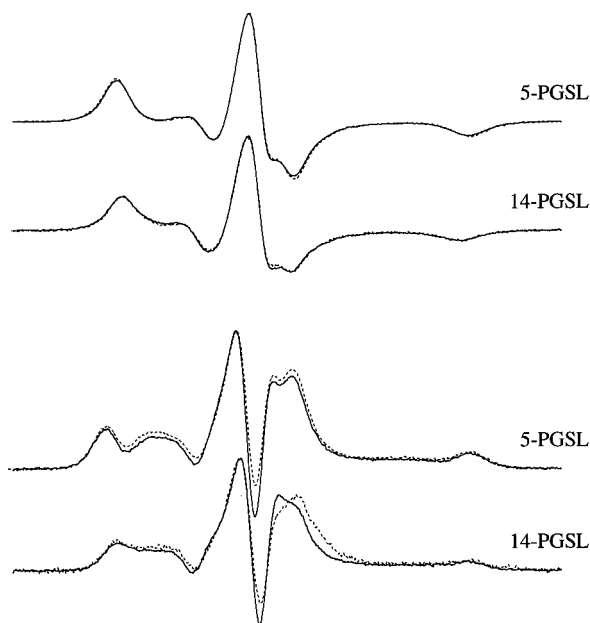
FIGURE 5: Conventional (top) and ST-EPR (bottom) spectra of cytochrome *c* oxidase/DMPG (1:46 mol/mol) complexes, doped with 5- or 14-PGSL (as indicated), in the absence (---) and presence (—) of 5 mM azide, at pH 7.4 and *T* = 10 °C. Spectra are normalized to the maximum positive line height for each pair. Total scan with = 100 G.

Table 3: Normalized ST-EPR Integrated Intensities and Effective T_1T_2 Relaxation Time Products from Progressive Saturation[a]

spin label	I_{ST} ($\times 10^2$)	$(T_1T_2)^{eff}$ ($\times 10^{14}$ s^2)
+Azide		
5-PGSL	0.45	4.8
14-PGSL	0.30	2.6
−Azide		
5-PGSL	0.33	2.7
14-PGSL	0.27	1.8

[a] I_{ST} values (defined in ref *24*) and $(T_1T_2)^{eff}$ values (obtained from power saturation curves according to eq 3) are given for the 5- and 14-PGSL spin labels in DMPG/cyt ox (43:1 mol/mol) complexes at 10 °C, in the presence and absence of 5 mM azide.

interface. Predominantly, the higher values of $I_{ST,P}$ arise from motional restriction of the lipid chains at the protein interface (cf. Table 1 and ref *24*). Additionally, however, T_1 relaxation enhancement by interaction with the paramagnetic metal centers in cytochrome *c* oxidase may also affect the ST-EPR intensities (see, e.g., ref *34*). The result of paramagnetic interactions is to reduce ST-EPR spectral intensities and therefore the degree of chain motional restriction may be greater than reflected by the measured values of $I_{ST,P}$.

Paramagnetic interactions with the metal centers of cytochrome oxidase have been investigated by reaction of azide. Azide is known to interact with the Cu_B^{2+} and heme a_3 cofactors (*2,36*). Therefore, the effect of azide on the spin−lattice relaxation rates of these metals can be used to detect paramagnetic contributions to the relaxation behavior of the spin-labeled lipids. Conventional and saturation transfer EPR spectra of the 5- and 14-PGSL spin labels in DMPG/cyt ox complexes of low lipid/protein ratio, in the presence and absence of azide, are given in Figure 5. Binding azide has practically no effect on the conventional EPR spectra of the spin-labeled lipids, because the metal ligands are not expected to affect the overall lipid−protein interactions. Some differences are observed in the line shapes of the ST-EPR spectra that are given in the lower part of Figure 5. The effects of modification of the spin state of the heme a_3 group, and/or bridging of the two metal centers, by the azide ligand (*36*) are seen much more clearly, however, in the ST-EPR intensities that are given in Table 3. Binding of azide to the metal ion centers will not change the mobility of the lipids associated with the protein (cf. upper part of Figure 5). Therefore, the differences in I_{ST} in the presence and absence of azide must arise from changes in efficiency of paramagnetic relaxation on modifying the spin state of the heme a_3 and/or Cu_B centers. Supporting evidence for this comes also from the effective relaxation time products, $(T_1T_2)^{eff}$, determined from progressive saturation experiments,

the values of which are also given in Table 3 (see later discussion). The direction of the change in both I_{ST} and $(T_1T_2)^{eff}$ is such that the paramagnetic relaxation enhancement is reduced on binding azide.

The ST-EPR intensities, I_{ST}, approximately are proportional to the effective spin−lattice relaxation times, T_1^{eff} (*35, 37*), and therefore the enhancements in paramagnetic relaxation rate are given by (see ref *34*)

$$\Delta(1/I_{ST}) = \frac{1}{I_{ST}} - \frac{1}{I_{ST}^0} \approx \left(\frac{T_1^0}{I_{ST}^0}\right)\frac{1}{T_1^P} \qquad (2)$$

where I_{ST}^0 and T_1^0 are the ST-EPR integral and effective T_1, respectively, in the absence of azide, and $1/T_1^P$ is the change in T_1 relaxation rate induced by azide. From Table 3, the effects of azide are characterized by $\Delta(1/I_{ST}) = -79$ and -36 for 5-PGSL and 14-PGSL, respectively. This suggests that the metal ion centers that are modified by azide are situated closer to the polar/apolar surface than to the middle of the membrane, i.e., closer to the C-5 position than to the C-14 position of the lipid chains (cf. ref *38*). Preliminary molecular modeling by arranging lipid fatty acid chains around the hydrophobic perimeter of the X-ray crystal structure of bovine cytochrome *c* oxidase (*1, 2*), with their vertical position determined by the transmembrane hydrophobic stretches identified in the cytochrome oxidase structure, agrees with this result. This also holds true for the location of the heme a_3−Cu_B^{2+} center relative to the chains of those phospholipids that are resolved in the crystal structure (*1*).

Progressive Saturation Experiments. Lipid−protein interactions and paramagnetic relaxation enhancements were also studied by means of progressive saturation of the conventional V_1 EPR spectra. The saturation curves for the integrated spectral intensity with increasing microwave radiation power are given in Figure 6. Data are presented for various *n*-PGSL spin labels in DMPG membranes and in DMPG/cyt ox complexes in the gel phase at 10 °C. Least strongly saturating are the spin labels in lipid membranes without protein (open symbols). Interaction with cytochrome oxidase increases the degree of saturation of the lipid spin labels, producing larger deviations from a linear dependence of the EPR intensity on H_1 field (solid symbols). Among the different spin-label positions, 7-PGSL stands out as saturating less readily both in DMPG membranes and in DMPG/cyt ox complexes. This pronounced relaxation enhancement, seen also above in the ST-EPR spectra, arises
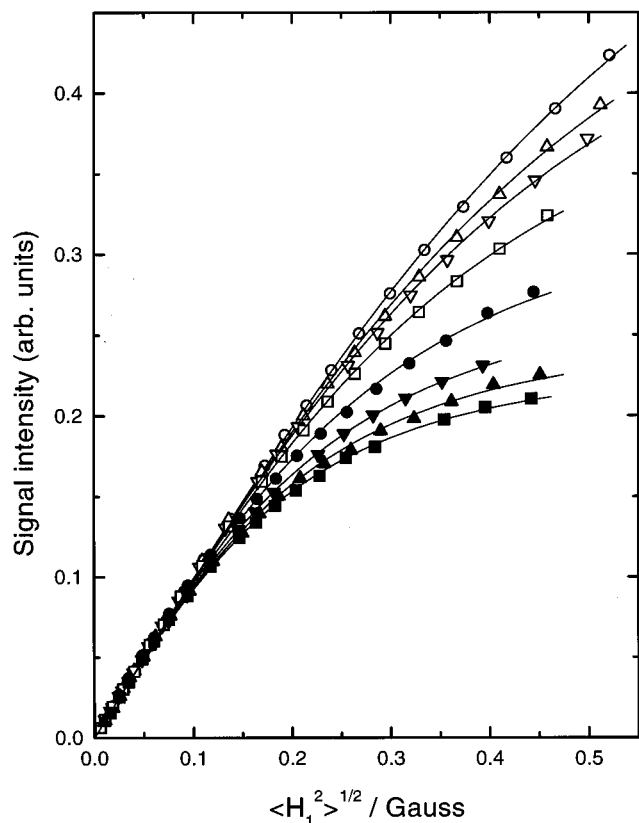
FIGURE 6: Progressive saturation of the second integral of V_1 EPR spectra from *n*-PGSL spin labels in DMPG dispersions (open symbols) and in cytochrome *c* oxidase/DMPG complexes (solid symbols). Saturation curves are given as a function of H_1 field for 5-PGSL ($\square$, $\blacksquare$), 7-PGSL ($\bigcirc$, $\bullet$), 12-PGSL ($\triangle$, $\blacktriangle$), and 14-PGSL ($\triangledown$, $\blacktriangledown$) positional isomers. Spectra were measured at 10 °C. Solid lines indicate least-squares fits to eq 3, with the fitting parameters given in Table 4.

from spin−spin interactions that result from partial exclusion of the 7-PGSL spin label in the lipid gel phase. For other positions of labeling, the degree of saturation increases systematically from the terminal methyl toward the head-group region of the lipid chains.

The power saturation curves for the integrated intensity, A, of the V_1 EPR spectra can be described by the following form for the dependence on H_1 field (*22*):

$$A(H_1) = \frac{A_0 H_1}{[1 + \gamma_e^2 H_1^2 (T_1 T_2)^{\text{eff}}]^{1/2}} \quad (3)$$

where T_1^{eff} and T_2^{eff} are the effective spin−lattice and spin−spin relaxation times, respectively, γ_e is the electron gyromagnetic ratio, and A_0 is a normalization constant. Fits of this equation to the data for DMPG membranes are given by the solid lines in Figure 6. Equation 3 gives an adequate description of the saturation behavior of these single-component spectra. Values of the effective $T_1 T_2$ relaxation time products, obtained from fitting the saturation curves, are given in Table 4. In general, the results of progressive saturation experiments parallel, and confirm, those from the ST-EPR intensities that are given in Table 2. Slight deviations are found in the relative values of $(T_1 T_2)^{\text{eff}}$ compared with those of I_{ST}, because the former depend not only on T_1^{eff} but also on T_2^{eff} (i.e., additionally on the line widths). In particular, the larger values of $(T_1 T_2)^{\text{eff}}$ for the DMPG/cyt

Table 4: Effective $T_1 T_2$ Relaxation Time Products from Progressive Saturation Measurements[a]

spin label	$(T_1 T_2)_{\text{P}}^{\text{eff}}$ ($\times 10^{14}$ s^2)	$(T_1 T_2)_{\text{L}}^{\text{eff}}$ ($\times 10^{14}$ s^2)
5-PGSL	5.7	1.6
7-PGSL	3.4	0.6
12-PGSL	5.1	0.9
14-PGSL	4.0	1.1

[a] $(T_1 T_2)^{\text{eff}}$ values (obtained from power saturation curves according to eq 3) are given for *n*-PGSL spin labels in DMPG membranes, $(T_1 T_2)_{\text{L}}^{\text{eff}}$, and in DMPG/cyt ox (53:1 mol/mol) complexes, $(T_1 T_2)_{\text{P}}^{\text{eff}}$, at 10 °C.

ox complexes imply slower rates of chain rotational motion, as is predicted theoretically for correlation times greater than $\tau_R \approx 10^{-8}$ s (*39*).

The values of $(T_1 T_2)^{\text{eff}}$ for DMPG/cyt ox complexes in the presence and absence of azide are given in Table 3 for the 5- and 14-PGSL spin labels. Binding of azide to the paramagnetic metal centers in cytochrome *c* oxidase corresponds to changes in relaxation rate of $\Delta(1/T_1 T_2) = -1.6 \times 10^{13}$ and -1.7×10^{13} s^{-2} for 5-PGSL and 14-PGSL, respectively, in the gel phase. Corrected for the different line widths, this corresponds to values of $\Delta(1/T_1^{\text{eff}}) = -3.2 \times 10^5$ and -2.7×10^5 s^{-1} for 5-PGSL and 14-PGSL. The relative values of the change in T_1 relaxation rate are therefore in agreement with the conclusion, reached already from the ST-EPR intensities, that the azide binding site, i.e., the heme a_3−Cu$_B^{2+}$ binuclear center, is closer to the 5-position than to the 14-position of the lipid chains.

CONCLUSIONS

Nonlinear EPR methods are found to be a sensitive means to investigate lipid−protein interactions in gel-phase membranes. These techniques are likely to be applicable not only to membranes reconstituted with synthetic lipids but also generally to any membrane system in which the lipid mobility is low, which is particularly the case when the protein component forms quasicrystalline arrays (e.g., refs *8* and *40*).

The lipid chains that interact directly with the hydrophobic transmembrane surface of cytochrome *c* oxidase are hindered in their rotational motion, relative to those in gel-phase membranes. This is seen by the increase in ST-EPR intensities and values of the effective relaxation time $T_1 T_2$ products (Tables 2 and 4). The effect of the transmembrane profile of the protein surface is seen very clearly, relative to the chain flexibility gradient present in gel-phase lipid membranes (Figure 3). The preferential increase in hindrance of the chain motion for spin labels close to the methyl terminal is consistent with the intramembrane structure of cytochrome *c* oxidase, which consists of polytopic α-helix bundles (*1*).

Proximity of the first shell of boundary lipids to the paramagnetic metal centers in cytochrome *c* oxidase is demonstrated directly by the effects on the spin−lattice relaxation of spin-labeled lipids. This relaxation enhancement is dipolar in origin, but estimates of distances are limited by uncertainties in the relaxation rates of the paramagnetic centers. The dependence on position of the spin label in the lipid chain, however, gives information on the vertical location of the azide binding site relative to the lipid

membrane that is fully in agreement with the crystal structure of the enzyme.

REFERENCES

1. Tsukihara, T., Aoyama, H., Yamashita, E., Tomizaki, T., Yamaguchi, H., Shinzawa-Itoh, K., Nakashima, R., Yaono, R., and Yoshikawa, S. (1996) *Science 272*, 1136−1144.
2. Yoshikawa, S., Shinizawa-Itoh, K., Nakashima, R., Yaono, R., Yamashita, E., Inoue, N., Yao, M., Fei, M. J., Libeu, C. P., Mizushima, T., Yamaguchi, H., Tomizaki, T., and Tsukihara, T. (1998) *Science 280*, 1723−1729.
3. Jost, P. C., Griffith, O. H., Capaldi, R. A., and Vanderkooi, G. (1973) *Proc. Natl. Acad. Sci. U.S.A. 70*, 480−484.
4. Knowles, P. F., Watts, A., and Marsh, D. (1979) *Biochemistry 18*, 4480−4487.
5. Knowles, P. F., Watts, A., and Marsh, D. (1981) *Biochemistry 20*, 5888−5894.
6. Powell, G. L., Knowles, P. F., and Marsh, D. (1987) *Biochemistry 26*, 8138−8145.
7. Marsh, D., and Horváth, L. I. (1998) *Biochim. Biophys. Acta 1376*, 267−296.
8. Páli, T., Finbow, M. E., Holzenburg, A., Findlay, J. B. C., and Marsh, D. (1995) *Biochemistry 34*, 9211−9218.
9. Bienvenue, A., Bloom, M., Davis, J. H., and Devaux, P. F. (1982) *J. Biol. Chem. 257*, 3032−3038.
10. Horváth, L. I., Brophy, P. J., and Marsh, D. (1993) *Biochim. Biophys. Acta 1147*, 277−280.
11. Horváth, L. I., Brophy, P. J., and Marsh, D. (1993) *Biophys. J. 64*, 622−631.
12. Kleinschmidt, J. H., Powell, G. L., and Marsh, D. (1998) *Biochemistry 37*, 11579−11585.
13. Marsh, D., and Watts, A. (1982) in *Lipid−Protein Interactions* (Jost, P. C., and Griffith, O. H., Eds.) Vol. 2, pp 53−126, Wiley-Interscience, New York.
14. Yu, C., Yu, L., and King, T. E. (1975) *J. Biol. Chem. 250*, 1383−1392.
15. Cable, M. B., and Powell, G. L. (1980) *Biochemistry 19*, 5679−5686.
16. Watts, A., Marsh, D., and Knowles, P. F. (1978) *Biochem. Biophys. Res. Commun. 81*, 403−409.
17. Lowry, O. H., Rosebrough, N. J., Farr, A. L., and Randall, R. J. (1951) *J. Biol. Chem. 193*, 265−275.
18. Rouser, G., Fleischer, S., and Yamamoto, A. (1970) *Lipids 5*, 494−496.
19. Yonetani, T. (1966) *Biochem. Prep. 11*, 14−20.
20. Fajer, P., and Marsh, D. (1982) *J. Magn. Reson. 49*, 212−224.
21. Hemminga, M. A., De Jaeger, P. A., Marsh, D., and Fajer, P. (1984) *J. Magn. Reson. 59*, 160−163.
22. Páli, T., Horváth, L. I., and Marsh, D. (1993) *J. Magn. Reson. A101*, 215−219.
23. Thomas, D. D., Dalton, L. R., and Hyde, J. S. (1976) *J. Chem. Phys. 65*, 3006−3024.
24. Horváth, L. I., and Marsh, D. (1983) *J. Magn. Reson. 54*, 363−373.
25. Marsh, D. (1999) *Methods Enzymol. 294* (Part C), 59−92.
26. Bartucci, R., Páli, T., and Marsh, D. (1993) *Biochemistry 32*, 274−281.
27. Pates, R. D., and Marsh, D. (1987) *Biochemistry 26*, 29−39.
28. Marsh, D., and Horváth, L. I. (1989) in *Advanced EPR. Applications in Biology and Biochemistry* (Hoff, A. J., Ed.) pp 707−752, Elsevier, Amsterdam.
29. Marsh, D., and Horváth, L. I. (1992) *J. Magn. Reson. 99*, 323−331.
30. Marsh, D. (1980) *Biochemistry 19*, 1632−1637.
31. Fajer, P., and Marsh, D. (1983) *J. Magn. Reson. 51*, 446−459.
32. Watts, A., and Marsh, D. (1981) *Biochim. Biophys. Acta 642*, 231−241.
33. Fajer, P., Watts, A., and Marsh, D. (1992) *Biophys. J. 61*, 879−891.
34. Marsh, D., Páli, T., and Horváth, L. I. (1998) in *Biological Magnetic Resonance*, *Vol. 14, Spin-Labeling: The Next Millennium* (Berliner, L. J., Ed.) Chapter 2, pp 23−82, Plenum Press, New York.
35. Marsh, D., and Horváth, L. I. (1992) *J. Magn. Reson. 97*, 13−26.
36. Hunter, D. J. B., Salerno, J. C., and Ingledew, W. J. (1998) *Biochim. Biophys. Acta 1364*, 55−62.
37. Páli, T., Livshits, V. A., and Marsh, D. (1996) *J. Magn. Reson. B113*, 151−159.
38. Páli, T., Bartucci, R., Horváth, L. I., and Marsh, D. (1992) *Biophys. J. 61*, 1595−1602.
39. Livshits, V. A., Páli, T., and Marsh, D. (1998) *J. Magn. Reson. 133*, 79−91.
40. Jost, P. C., McMillen, D. A., Morgan, W. D., and Stoeckenius, W. (1978) in *Light Transducing Membranes* (Deamer, D., Ed.) pp 141−154, Academic Press, New York, San Francisco, and London.